

Magneto-optical Kerr effects of half-metallic ferromagnetic transition metal chalcogenides in zinc-blende and wurtzite structures

Hongming Weng,^{1,*} Yoshiyuki Kawazoe,¹ and Jinming Dong²

¹*Institute for Materials Research, Tohoku University, Sendai 980-8577, Japan*

²*Group of Computational Condensed Matter Physics, National Laboratory of Solid State Microstructures and Department of Physics, Nanjing University, Nanjing 210093, People's Republic of China*

(Received 12 March 2006; revised manuscript received 28 June 2006; published 11 August 2006)

The electronic structure and polar magneto-optical Kerr effect (MOKE) of the transition metal chalcogenides, such as CrSe, CrTe, and VTe, in zinc-blende and wurtzite structures are studied by full-potential density-functional calculations. The p - d exchange interaction in these half-metallic ferromagnets is estimated and found to be ferromagnetic. The MOKE is quite large in all of these compounds. It is found that the peaks in Kerr rotation spectra lower than 3.0 eV are enhanced by the plasma resonance due to the metallic feature in the majority spin channel, while those higher than 3.0 eV originate from the quite large off-diagonal optical conductivity element. The CrTe exhibits a larger Kerr effect than the CrSe since the spin-orbit coupling of p orbitals in Te is stronger than that in Se, while the larger Kerr effect in VTe than in CrTe is quite unexpected because the magnetic moment in VTe is smaller than in CrTe. This strange result is understood in terms of transitions from the underlying band structure. Our calculations can give hints to the understanding of MOKE and the design of the new materials with technologically desirable magneto-optical properties through tailoring their electronic band structures.

DOI: [10.1103/PhysRevB.74.085205](https://doi.org/10.1103/PhysRevB.74.085205)

PACS number(s): 75.50.Pp, 78.20.Ls, 75.30.Et

I. INTRODUCTION

Diluted magnetic semiconductors (DMSs) have been intensively studied due to their interesting magnetic, electronic, and optical properties.¹ In DMSs, the transition metal ions substitute for the cations of host semiconductor, acting as spin injectors. The d orbital of the transition metal ion mixes with the p orbital of the neighboring anion, which strongly influences the valence band of the semiconductor. The s orbital of the conduction band will also be influenced by the magnetic ion though the interaction between them is much smaller. These couplings between the magnetic ion and charge carriers are the so-called s , p - d exchange interaction in DMSs. Its most important feature is the spin-polarized interaction, causing the interesting physical properties of DMSs.² One direct result of the s , p - d exchange interaction is the giant Zeeman splitting of the host bands, leading to quite large magneto-optical (MO) effects in DMSs. Therefore magneto-optic measurement plays an important role in clarifying the s , p - d exchange interaction and electronic structures of DMSs.^{3,4} Besides this, the potential applications of the MO effects in the magneto-optic disks for data storage,⁵ optical isolators, and circulators for optical communications⁶ also stimulate the intense experimental studies of the MO effects in DMSs. On the other hand, there are less theoretical works, especially *an initio* calculations of MO effects in DMSs,⁷ because the electronic structure of the low concentration doped system is quite complex, making the calculations of it and MO effects much suffering. But the characteristic s , p - d exchange interaction, parametrized as $N_0\alpha$ (s - d) and $N_0\beta$ (p - d) in the mean-field model,^{8,9} is nearly independent of the concentration of doped transition metal, which could be extracted from calculation of the spin polarized band structure on a hypothetical 100% doping system^{7,9,10} though the impurity bands and other low-

concentration-doped effects could not be included in this case compared with the real DMS systems.

Recently, the room-temperature ferromagnetic DMS $\text{Zn}_{1-x}\text{Cr}_x\text{Te}$ was discovered and its p - d exchange interaction $N_0\beta$ was found to be ferromagnetic by an analysis of the magnetic circular dichroism spectrum.¹¹ Xie *et al.* found that the Zinc-blende (ZB) phase of CrTe, the end limit of $\text{Zn}_{1-x}\text{Cr}_x\text{Te}$ with $x=1$, is half-metallic ferromagnets and is predicted to be stable mechanically.¹² They further found that CrSe, CrTe, and VTe are all half metals both in the ZB and wurtzite (WZ) structures.^{12,13} The half-metallic ferromagnets are believed to have unusual MO effects since they are metallic for majority spin electrons, but insulating for minority ones, which will naturally give rise to extraordinary magnetotransport and optical properties. At the same time, the half-metallic ferromagnets are thought as the ideal materials for high performance spintronic devices due to their 100% spin polarization. Especially those in the ZB or WZ phase are compatible in structure with the important III-V or II-VI semiconductors, which would have high efficiency in spin injection.¹⁴ So, a combined study of the p - d exchange interaction and MO effects is highly desired, which would be very helpful in understanding the p - d exchange interaction and large MO effects in the DMSs and also in designing new multifunctional materials.

In this paper we will employ an accurate full-potential density-functional method to systematically study a series of half-metallic V and Cr chalcogenides (mainly Se and Te) both in the ZB and WZ structures. The band structure and the polar magneto-optical Kerr effect (MOKE) for each compound are calculated. The neighborhood of V and Cr, Se and Te in the periodic table would be good for studying the systematical changes in electronic structure and MOKE. The p - d exchange interaction is found to be positive, i.e., ferromagnetic, being consistent with that in $\text{Zn}_{1-x}\text{Cr}_x\text{Te}$. The

MOKE is found to be quite large in all of these compounds. Two kinds of contributions to MOKE are identified. The simple band structure in highly symmetrical ZB structure makes the understanding of difference in MOKE spectra very easy and convenient.

II. METHODOLOGY

The highly accurate all electron full-potential linearized augmented plane-wave method implemented in WIEN2K (Ref. 15) is used for electronic structure calculations within the generalized gradient approximation (GGA).¹⁶ The lattice parameters of CrSe, CrTe, and VTe in the ZB and WZ structures are taken from Refs. 12 and 13. The spin-orbit coupling (SOC) is taken into account by using the second-variation method¹⁷ self-consistently. The cutoff energy for the included eigenstates is as high as 2.5 Ryd. A separated calculation with cutoff energy of 3.5 Ryd gives nearly the same results. The efficiency of the second-variation approach to treat SOC in WIEN2K has been demonstrated in Ref. 18, which showed that the calculated spin-orbit splitting in Te compounds by the WIEN2K code is well consistent with its experimental data, even without including the $p_{1/2}$ local orbital corrections. In our calculations, the magnetization is taken along [001] direction for both ZB and WZ structures when the SOC is included. In such configurations, the polar Kerr effect is given by the well-known formula for the complex Kerr angle in the two-media approach,^{19,20}

$$\theta_K(\omega) + i\varepsilon_K(\omega) = \frac{-\sigma_{xy}(\omega)}{\sigma_{xx}(\omega) \sqrt{1 + \frac{4i\pi}{\omega} \sigma_{xx}(\omega)}}, \quad (1)$$

with $\theta_K(\omega)$ the Kerr rotation angle and $\varepsilon_K(\omega)$ the so-called Kerr ellipticity. This macroscopical model formula has been widely and successfully used in calculation of MOKE spectra for many systems, such as element metals, simple or complex structured compounds, and even multilayered systems.²⁰⁻²² $\sigma_{\alpha\beta}$ ($\alpha, \beta \equiv x, y, z$) is the element of optical conductivity tensor, which is calculated within the electric-dipole approximation using the Kubo linear-response formula:²¹

$$\sigma_{\alpha\beta}(\omega) = \frac{ie^2}{m^2 \hbar V} \sum_k \sum_{j,j'} \frac{f(E_{jk}) - f(E_{j'k})}{\omega_{jj'}} \times \left[\frac{\Pi_{j'j}^\alpha \Pi_{jj'}^\beta}{\omega - \omega_{jj'} + i/\tau} + \frac{(\Pi_{j'j}^\alpha \Pi_{jj'}^\beta)^*}{\omega + \omega_{jj'} + i/\tau} \right]. \quad (2)$$

Here, $f(E_{jk})$ is the Fermi function, $\hbar\omega_{jj'} = E_{jk} - E_{j'k}$ is the energy difference of the Kohn-Sham energies E_{jk} , and τ^{-1} is the inverse of the lifetime of excited Bloch electron states, taken as 0.4 eV, which is thought to be large enough for the transition metal compounds.²² The $\Pi_{j'j}^\alpha$ are the elements of the dipole optical transition matrix. There are two ways of calculating the complex optical conductivity tensor. One is to use directly Eq. (2), and the other is first to calculate the absorptive parts of the tensor and then the dispersive parts could be obtained by the Kramers-Kronig relations²¹ be-

tween both parts. Here, we use the first method to avoid the possible error or inaccuracy brought by the Kramers-Kronig transformation since the MO effect is a very small quantity which is related to the difference between responses to the left- and right-hand circularly polarized light. There are totally about 20 000 k points sampled in the Brillouin zone for the integration over k space in the self-consistent calculation, which is assumed to be converged once the integrated charge density difference per formula unit, $\int |\rho_n - \rho_{n-1}| dr$, is less than 0.0001, where $[\rho_{n-1}]$ and $[\rho_n]$ represent the input and output charge density, respectively. This number of k points is also used to get the self-consistent potential in calculations of the anomalous Hall effect of bcc Fe metal.²³ In order to get the accurate optical conductivity tensor, more dense k -space sampling, as many as 50 000 k points, is used, and the special k -point method is adopted for evaluating Eq. (2). The upper limit of the band index j and j' is taken as the band lying at as high as 2.5 Ryd above Fermi level, and the convergence is carefully checked by varying it from 1.5 to 3.5 Ryd.

Because of the metallic nature, the intraband transitions will have a dominant contribution to the optical tensor in the lower-energy region. This kind of contribution to the diagonal components of the conductivity tensor is usually described by the Drude formula,

$$\sigma_{\alpha\alpha}^D(\omega) = \frac{\omega_{P,\alpha}^2}{4\pi \left(\frac{1}{\tau_D} - i\omega \right)}, \quad (3)$$

where $\omega_{P,\alpha}$ is the unscreened plasma frequency and τ_D is the phenomenological Drude electron relaxation time, characterizing the scattering of charge carriers, which depends on the amount of defects, and therefore varies from sample to sample. τ_D is different from the interband relaxation time parameter τ . The τ can be frequency dependent²⁴ and should be nonzero since excited states always have a finite lifetime, whereas τ_D will approach zero for very pure materials. It is shown that in the similar half-metallic systems a τ_D^{-1} of about 0.3 eV can well reproduce the experimental spectra.²⁵ We have calculated the plasma frequency ω_p by

$$\omega_{P,\alpha}^2 = \frac{4\pi e^2}{m^2 V} \sum_{jk} \delta(E_{jk} - E_F) |\Pi_{jj}^\alpha|^2. \quad (4)$$

After that, it is found that the Drude type intraband contribution to the MOKE is small in the lower-energy region (<2.0 eV) and has nearly no effects in the higher-energy range.

III. RESULT AND DISCUSSION

The band structures of CrSe, CrTe, and VTe in the ZB phase are shown in Fig. 1. Those in the WZ phase (not shown) have similar features as in the ZB case. The spin polarized band structures in the left-hand panels of Fig. 1 are calculated without SOC. Compared with those calculated with SOC, it is obvious that the half-metallic feature is stable in all the compounds no matter whether SOC is included or

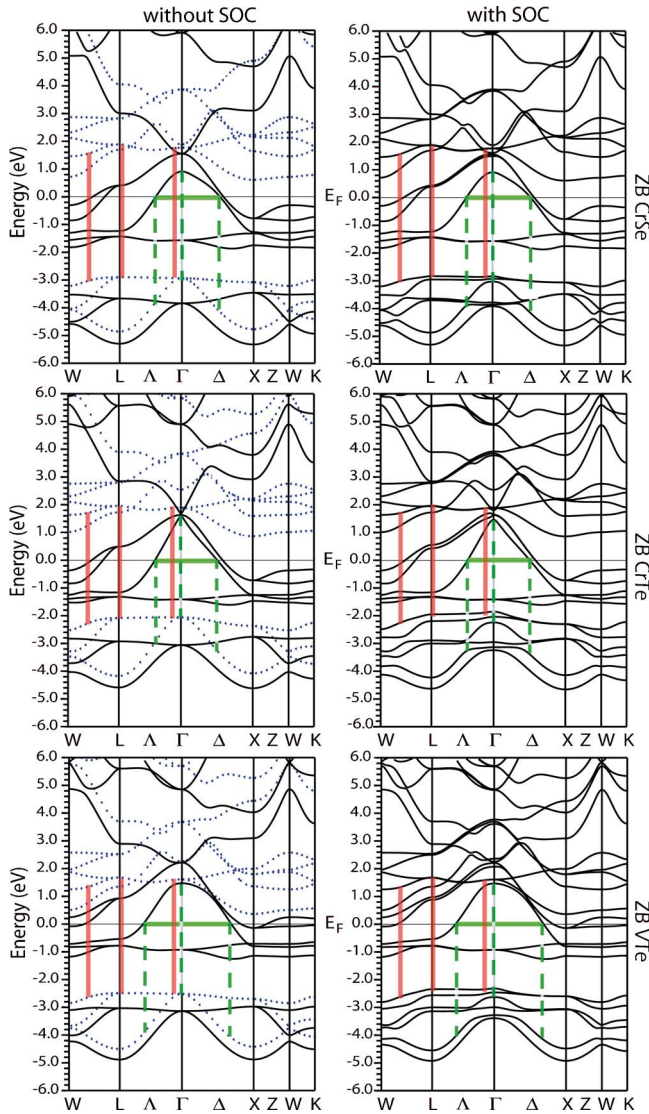


FIG. 1. (Color online) The band structures of CrSe (upper panels), CrTe (middle panels), and VTe (lower panels) in their ZB structures, calculated without (left-hand panels) and with (right-hand panels) the spin-orbit coupling (SOC). The vertical solid and dashed lines indicate the different possible transitions from band to band. In the left-hand panels, the solid line is for band structure of the majority spin (spin-up) electrons, while the dotted line is for those of the minority spin (spin-down) ones.

not. The p - d exchange interaction makes the p bands (ranging from -2.0 to -6.0 eV) of Se or Te spin split. At the center of the Brillouin zone (Γ point), the spin splitting energies (Δ) of the valence p bands are about 1.0, 1.0, and 0.56 eV for CrSe, CrTe, and VTe, respectively. The local magnetic moment on Cr or V atoms in CrSe, CrTe, and VTe are 3.721 , 3.759 , and $2.675\mu_B$, respectively. The p - d exchange interaction is usually described by⁹

$$H_{p-d} = -N_0\beta \cdot x\vec{S} \cdot \vec{s}, \quad (5)$$

where x is the doping concentration of transition metal, and \vec{S} and \vec{s} are the spin operators of the transition metal electrons

in the d states and the valence band, respectively. After knowing these, we can estimate the p - d exchange interaction parameter $N_0\beta$ of these systems in the same manner as done for MnTe,⁹ MnSe, and MnAs.¹⁰ It is found that $N_0\beta$ is 0.537, 0.532, and 0.419 eV for CrSe, CrTe, and VTe, respectively. All the $N_0\beta$ parameters are found to be positive, i.e., the p - d exchange interaction is ferromagnetic, inconsistent with the experimental values in $\text{Zn}_{1-x}\text{Cr}_x\text{Se}$,²⁶ and $\text{Zn}_{1-x}\text{Cr}_x\text{Te}$.¹¹ It is in sharp contrast to the negative value in the cases of MnTe, MnSe, and MnAs,^{9,10} which could be ascribed to their band-structure difference. According to the Schrieffer-Wolff formula,^{2,9,27} the sign of $N_0\beta$ is determined by the energy position of the donor (occupied) local d level relative to the top of the valence p orbitals. Here, the occupied $3d$ orbitals of Cr or V are higher in energy than the top of Se or Te p orbitals, while those of Mn $3d$ orbitals are lower in the case of MnTe, MnSe, or MnAs.^{9,10,27} In fact, here, the ferromagnetic (FM) p - d exchange interaction is possible because Cr or V is less than half filled with both spin-up and -down orbitals empty. So, it is possible for the p electrons to make the virtual jump in both channels. According to Hund's first rule, the virtual jump of the electrons with their spins parallel to those on the local d orbital, i.e., the FM kinetic exchange interaction, is preferable in energy. For the half filled or more than half filled ions, such as Mn, Fe, and Co in II-VI semiconductors, only spin-down orbitals are empty while the local magnetic moment comes from the unpaired spin-up electrons, making the FM channels forbidden for the virtual jump of electrons. But one exception is Co in TiO_2 . There, the Co ion is in its low-spin state,^{7,28} in which both spin-up and -down orbitals are not fully occupied, making the FM p - d exchange interaction possible and prevail over the antiferromagnetic (AFM) interaction. Also, the occupied Co d level is higher in energy than the top of valence oxygen p orbitals.⁷

In the pure ZB phase of ZnSe and ZnTe semiconductors, including SOC will split the sixfold degenerated (counting also the spin) highest energy valence-band state at Γ point into the twofold ($\Gamma_7, p_{1/2}$) and fourfold ($\Gamma_8, p_{3/2}$) substates. But in the cases of CrSe, CrTe, and VTe, the spin polarized p - d exchange interaction will modify this picture by further removing the remaining degeneracy, as shown in the right-hand panel of Fig. 1. It is obvious to see the spin-orbit splitting in the p bands of Se or Te, especially along the k paths from W to L and L to Γ . We can also easily find from the band structures that the spin splitting Δ induced by the p - d exchange interaction is larger than the spin-orbit splitting ξ in this 100% doping case, which is different from the picture² in the lower doping concentrations where $\Delta < \xi$ because Δ is proportional to x in Eq. (5). The p bands of Se or Te are first split into two subbands with energies 0 and Δ , respectively. The SOC then further split the triply degenerated subbands into three bands by keeping one fixed and other two shifted by $\xi/3$. Thus the six states now are $-\xi/3, 0, \xi/3, \Delta - \xi/3, \Delta, \Delta + \xi/3$.^{10,29} So, the estimated spin-orbit splitting at Γ point of Se and Te p bands is 0.33 and 0.50 eV, respectively. Both of them are smaller than those 0.38 and 0.85 eV, obtained for ZnSe and ZnTe, respectively, due to the strong p - d hybridization which reduces the effective SOC accordingly.^{10,18,29} It is also interesting that the t_{2g}

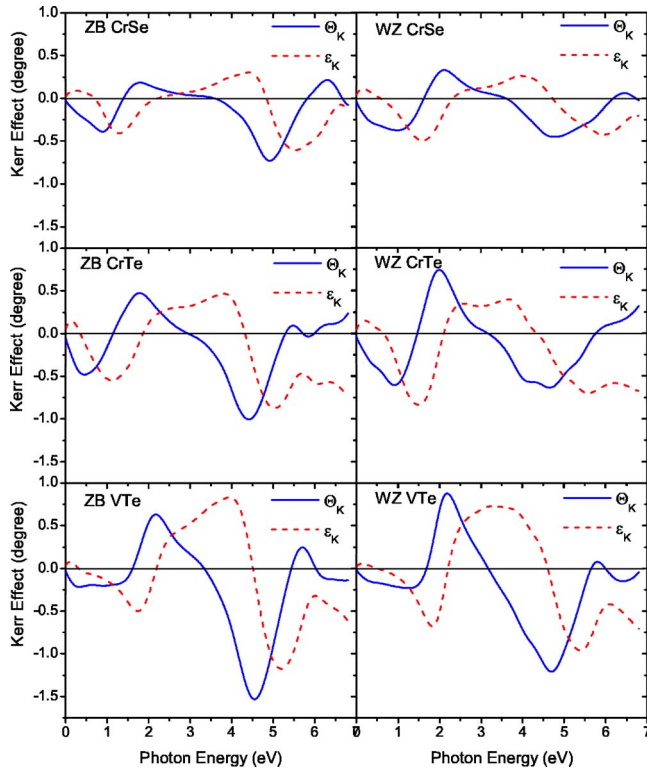


FIG. 2. (Color online) Calculated Kerr rotation (θ_K , solid line) and Kerr ellipticity (ϵ_K , dashed line) spectra for CrSe, CrTe, and VTe in the ZB (left panel) and WZ (right panel) structures.

bands of tetragonally coordinated Cr or V is affected by SOC while the e_g bands seem to be nearly unaffected, which is apparently shown by the bands along the Λ k path.

The calculated MOKE of these compounds in both ZB and WZ structures is presented in Fig. 2. All of them have quite large Kerr effect; even the moderately large lifetime broadening parameter of 0.4 eV is used in calculations. A smaller broadening parameter would increase the peak values. The Kerr rotation and the ellipticity are well compatible with each other. It is clearly seen that when the Kerr ellipticity crosses the zero line, a peak always appears in the Kerr rotation spectra and vice versa due to the Kramers-Kronig relations, which means our direct calculation of Eq. (2) is quite good. Though the peak value and position are somewhat different, as a whole, the shape of the spectra are quite similar due to the comparability of the electronic structures. Two kinds of structures in the Kerr rotation spectra are noticeable. One of them is lower than 3.0 eV, and another is higher than 3.0 eV. In the former, the peak around 2.0 eV becomes narrower and higher when the compound's structure changes from the ZB to WZ. Contrarily, in the latter, the Kerr rotation peak around 4.5 or 5.0 eV in the ZB phase undergoes broadening and lowering in the WZ phase. The quite large Kerr rotation near 2.0 eV and 4.5–5.0 eV would find possible applications of these compounds in the orange or ultraviolet laser light MO effect devices. The sensitivity of Kerr effect to the geometrical structure has already been used to detect the structure of thin films. Generally, the MOKE peaks in CrTe are larger than those in CrSe, which could be ascribed to the stronger SOC in Te than in Se. But it is quite

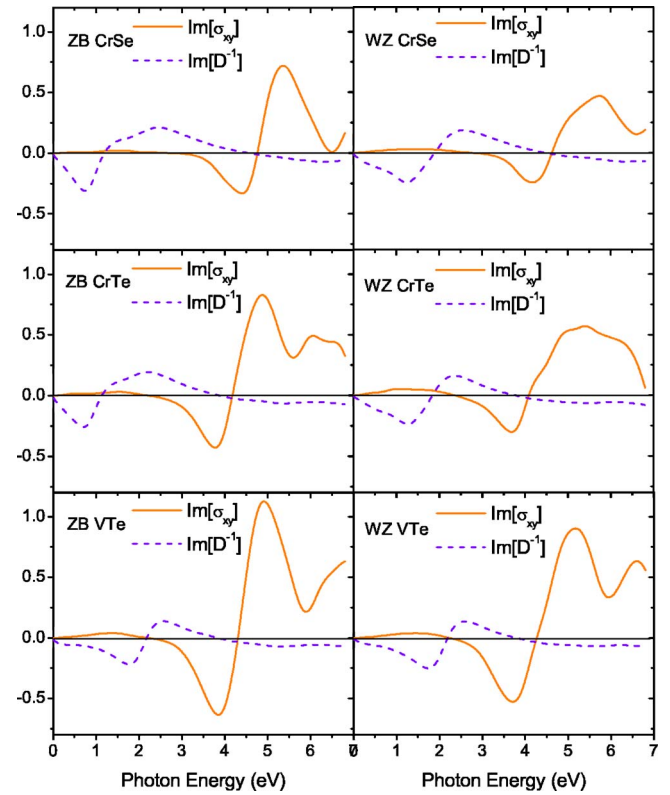


FIG. 3. (Color online) Separate contributions to the Kerr rotation spectra of CrSe, CrTe, and VTe in the ZB (left panel) and WZ (right panel) structures from $\text{Im}[\sigma_{xy}]$ (solid line) and $\text{Im}[D^{-1}]$ (dashed line).

strange to have the greater MOKE peaks in VTe than in CrTe because usually it is expected that the larger magnetic moment would bring the larger MO effect when the SOC is nearly the same, just as in the case of MnBi and CrBi.³⁰

To investigate the origin of Kerr spectra and understand the larger Kerr effect in VTe, let us consider the separate contributions of the numerator $\sigma_{xy}(\omega)$ and the denominator $D(\omega) \equiv \sigma_{xx}(\omega) \sqrt{1 + \frac{4i\pi}{\omega} \sigma_{xx}(a)}$ in Eq. (1) to the Kerr rotation angle in these systems. As shown in Fig. 3, the imaginary part of the inverse denominator, $\text{Im}[D^{-1}]$, exhibits a similar structure to the Kerr rotation spectrum in the energy region lower than about 3.0 eV, while the imaginary part of the off-diagonal optical conductivity, $\text{Im}[\sigma_{xy}]$, is very small in the same region, showing no such structure. On the contrary, in the energy region higher than 3.0 eV, the $\text{Im}[\sigma_{xy}]$ contributes most to the Kerr rotation spectra while the $\text{Im}[D^{-1}]$ keeps nearly a small constant. So, it is obvious that there exist different mechanisms for the Kerr rotation peaks in the lower and higher energy regions. The former is induced by the plasma resonance, confirming the idea of Feil and Haas³¹ based on model calculations for some magnetic metallic rare-earth or transition metal compounds. The latter mostly originates from the off-diagonal conductivity due to the interband transitions between the SOC-split bands. So, it would be easier to understand the calculated Kerr spectra in Fig. 2 by identifying the contributions of each band to the off-diagonal optical conductivity element. As shown in the left-hand panel of Fig. 1, the solid vertical lines indicate the

contributions near the absorption edge in the semiconducting spin-down channel. Around the absorption edge, the $\text{Im}[\sigma_{xy}]$ has the quite large peak structures. The dashed vertical lines indicate the transitions with the same transition energy, but should be forbidden because spin flip is not allowed in the dipole-approximation without SOC. When the SOC is taken into account, the spin-up and -down states are mixed to each other, and the initial p bands now have the large spin-orbit splitting, which will cause a large difference in the absorption of the circular polarized photons since it requires a change of the band's orbital angular momenta by \hbar or $-\hbar$. The transitions indicated by vertical dashed lines now are possible, as shown in the right panel of Fig. 1. Since these bands are all nearly parallel, the transitions between them should contribute a great weight to the absorption due to the well-known parallel-band effects.³² We noticed that VTe has one less valence electron than CrTe or CrSe, and so, its Fermi level is shifted downward compared with those of CrTe or CrSe, which makes much more part in k space be able to contribute to the transitions indicated by the dashed lines. As a result, VTe would have the larger $\text{Im}[\sigma_{xy}]$ and so the larger Kerr rotation than CrTe or CrSe. It seems that the larger magnetic moment or exchange splitting would not guarantee the larger MO effects. The detailed electronic structure probably plays more important role in the MO effects, determining the contributions of possible transitions to the diagonal and off-diagonal conductivities.

IV. CONCLUSION

In summary, the electronic structures and the polar MOKE spectra of half-metallic ferromagnetic transition

metal chalcogenides of CrSe, CrTe, and VTe in the ZB and WZ structures are studied by full-potential density-functional theory calculations. The p - d exchange interaction parameters $N_0\beta$ of these systems are estimated from the spin-polarized band structures and found to be ferromagnetic, being consistent with that in the room-temperature ferromagnetic DMS $\text{Zn}_{1-x}\text{Cr}_x\text{Te}$. The effective SOC of Se or Te in these systems is reduced by the strong p - d hybridization and is critical to the MO effects. The polar Kerr rotation is found to be quite large in the systems. Especially in the ZB VTe, the largest Kerr rotation angle is found to be as large as 15° around 4.5 eV, which lies in the ultraviolet energy range. The Kerr effect lower than 3.0 eV is enhanced by the plasma resonance due to the metallic feature in majority spin channel while that higher than 3.0 eV is caused by the large off-diagonal conductivity element contributed by the interband transitions between the spin-orbit split bands. We find that the larger Kerr effect in CrTe than in CrSe is due to the stronger SOC in Te than in Se, while the unusual larger Kerr effect in VTe than in CrTe is found to be caused by the unique difference between their electronic structures. We hope our calculations could give some hints to the understanding of MOKE and the design of the new materials with technologically desirable magneto-optical properties through tailoring their electronic band structures.

ACKNOWLEDGMENTS

The authors thank the staff of the Center for Computational Materials Science at the IMR for their support and the use of Hitachi SR8000/64 supercomputing facilities. H.W. acknowledges the help from Bang-Gui Liu in calculations.

*Corresponding author. Email address: hongming@imr.edu

¹*Diluted Magnetic (Semi-magnetic) Semiconductors*, edited by R. L. Aggarwal, J. K. Furdyna, and S. von Molnar, MRS Symposia Proceedings No. 89, Mater. Res. Soc. Symp. Proc. (Materials Research Society, Pittsburgh, 1987); *Diluted Magnetic Semiconductors*, edited by M. Jain (World Scientific, Singapore, 1991).

²K. Ando, in *Magneto-Optics*, Springer Series in Solid-State Science Vol. 128, edited by S. Sugano and N. Kojima (Springer, Berlin, 2000), Chap. 6.

³K. Ando, cond-mat/0208010 (unpublished); K. Ando, H. Saito, V. Zayets, and M. C. Debnath, J. Phys.: Condens. Matter **16**, S5541 (2004).

⁴T. Fukumura, Y. Yamada, K. Tamura, K. Nakajima, T. Aoyama, A. Tsukazaki, M. Sumiya, S. Fuke, Y. Segawa, T. Chikyow, T. Hasegawa, H. Koinuma, and M. Kawasaki, Jpn. J. Appl. Phys., Part 2 **42**, L105 (2003); Y. Yamada, H. Toyosaki, A. Tsukazaki, T. Fukumura, K. Tamura, Y. Segawa, K. Nakajima, T. Aoyama, T. Chikyow, T. Hasegawa, H. Koinuma, and M. Kawasaki, J. Appl. Phys. **96**, 5097 (2004); H. Toyosaki, T. Fukumura, Y. Yamada, and M. Kawasaki, Appl. Phys. Lett. **86**, 182503 (2005).

⁵M. Kaneko, in *Magneto-Optics*, Springer Series in Solid-State Science Vol. 128, edited by S. Sugano and N. Kojima (Springer, Berlin, 2000), Chap. 9.

⁶K. Ando, Proc. SPIE **1126**, 58 (1989).

⁷Hongming Weng, Jinming Dong, T. Fukumura, M. Kawasaki, and Y. Kawazoe, Phys. Rev. B **73**, 121201(R) (2006).

⁸T. Dietl, H. Ohno, F. Matsukura, J. Cibert, and D. Ferrand, Science **287**, 1019 (2002).

⁹B. E. Larson, K. C. Hass, H. Ehrenreich, and A. E. Carlsson, Phys. Rev. B **37**, 4137 (1988); Małgorzata Wierzbowska, Daniel Sanchez-Portal, and Stefano Sanvito, *ibid.* **70**, 235209 (2004).

¹⁰G. Theurich and N. A. Hill, Phys. Rev. B **66**, 115208 (2002).

¹¹H. Saito, V. Zayets, S. Yamagata, and K. Ando, Phys. Rev. Lett. **90**, 207202 (2003); Hongming Weng, Jinming Dong, T. Fukumura, M. Kawasaki, and Y. Kawazoe (unpublished).

¹²W. H. Xie, Y. Q. Xu, B. G. Liu, and D. G. Pettifor, Phys. Rev. Lett. **91**, 037204 (2003).

¹³W. H. Xie, B. G. Liu, and D. G. Pettifor, Phys. Rev. B **68**, 134407 (2003).

¹⁴G. Schmidt, D. Ferrand, L. W. Molenkamp, A. T. Filip, and B. J. van Wees, Phys. Rev. B **62**, R4790 (2000).

¹⁵P. Blaha, K. Schwarz, G. K. H. Madsen, D. Kvasnicka, and J. Luitz, WIEN2K, An Augmented Plane Wave+Local Orbitals Program for Calculating Crystal Properties (Karlheinz Schwarz, Techn. Universität, Wien, Austria, 2001).

¹⁶J. P. Perdew, K. Burke, and M. Ernzerhof, Phys. Rev. Lett. **77**, 3865 (1996).

- ¹⁷D. D. Koelling and B. N. Harmon, *J. Phys. C* **10**, 3107 (1977); A. H. MacDonald, W. E. Pickett, and D. D. Koelling, *ibid.* **13**, 2675 (1980).
- ¹⁸P. Carrier and S. H. Wei, *Phys. Rev. B* **70**, 035212 (2004).
- ¹⁹W. Reim and J. Schoenes, in *Magneto-Optical Spectroscopy of f-Electron Systems*, edited by K. H. J. Buschow and E. P. Wohlfarth (North-Holland, Amsterdam, 1990), Vol. 5, Chap. 2, p. 133; A. Vernes, L. Szunyogh, and P. Weinberger, *Phys. Rev. B* **65**, 144448 (2002); **66**, 214404 (2002).
- ²⁰V. N. Antonov, P. M. Oppeneer, A. N. Yaresko, A. Ya. Perlov, and T. Kraft, *Phys. Rev. B* **56**, 13012 (1997).
- ²¹H. Ebert, *Rep. Prog. Phys.* **59**, 1665 (1996).
- ²²P. M. Oppeneer, T. Maurer, J. Sticht, and J. Kübler, *Phys. Rev. B* **45**, 10924 (1992); V. N. Antonov, A. N. Yaresko, A. Ya. Perlov, V. V. Nemoshkalenko, P. M. Oppeneer, and H. Eschrig, *Low Temp. Phys.* **25**, 387 (1999) [*Fiz. Nizk. Temp.* **25**, 527 (1999)].
- ²³Y. Yao, L. Kleinman, A. H. MacDonald, J. Sinova, T. Jungwirth, D. S. Wang, E. Wang, and Q. Niu, *Phys. Rev. Lett.* **92**, 037204 (2004).
- ²⁴A. Santoni and F. J. Himpsel, *Phys. Rev. B* **43**, 1305 (1991).
- ²⁵R. Vidya, P. Ravindran, A. Kjekshus, and H. Fjellvåg, *Phys. Rev. B* **70**, 184414 (2004).
- ²⁶W. Mac, Nguyen The Khoi, A. Twardowski, J. A. Gaj, and M. Demianiuk, *Phys. Rev. Lett.* **71**, 2327 (1993).
- ²⁷A. K. Bhattacharjee, *Phys. Rev. B* **49**, 13987 (1994); P. Kacman, *Semicond. Sci. Technol.* **16**, R25 (2001).
- ²⁸Hongming Weng, Xiaoping Yang, Jinming Dong, H. Mizuseki, M. Kawasaki, and Y. Kawazoe, *Phys. Rev. B* **69**, 125219 (2004); Rebecca Janisch and Nicola A. Spaldin, *ibid.* **73**, 035201 (2006).
- ²⁹Jin-Cheng Zheng and James W. Davenport, *Phys. Rev. B* **69**, 144415 (2004).
- ³⁰P. M. Oppeneer, V. N. Antonov, T. Kraft, H. Eschrig, A. N. Yaresko, and A. Ya. Perlov, *J. Appl. Phys.* **80**, 1099 (1996).
- ³¹H. Feil and C. Haas, *Phys. Rev. Lett.* **58**, 65 (1987); J. Schoenes and W. Reim, *ibid.* **60**, 1988 (1988); H. Feil and C. Haas, *ibid.* **60**, 1989 (1988).
- ³²H. Ehrenreich, H. R. Philipp, and B. Segall, *Phys. Rev.* **132**, 1918 (1963); Walter A. Harrison, *ibid.* **147**, 467 (1966).